SUPPLEMENTAL FIGURES

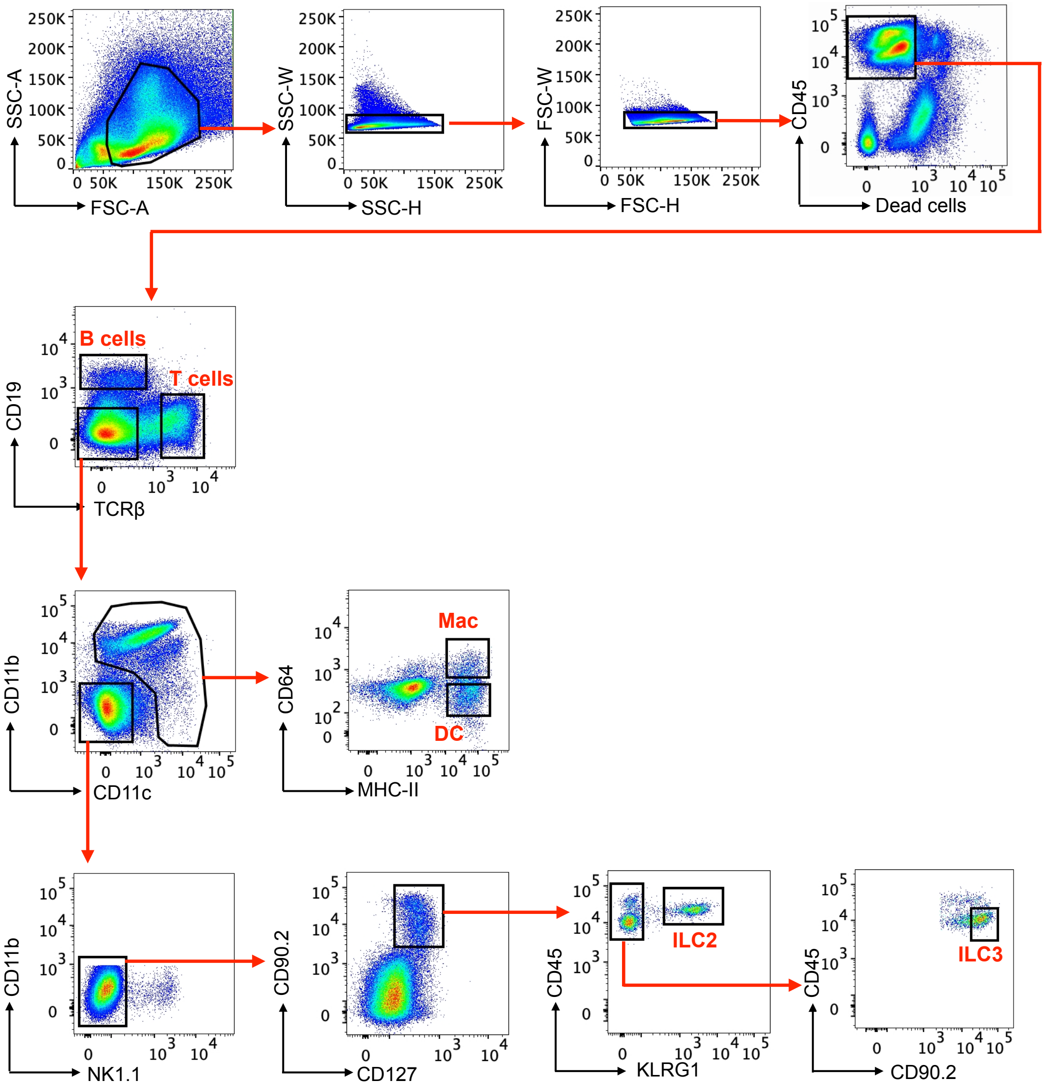

Figure S1. Gating strategy for sorting immune cells from the small intestine of C57BL/6 mice. A defined gating strategy was employed for sorting immune cell populations from the small intestine, including B cells, T cells, macrophages, dendritic cells, ILC2 and ILC3.

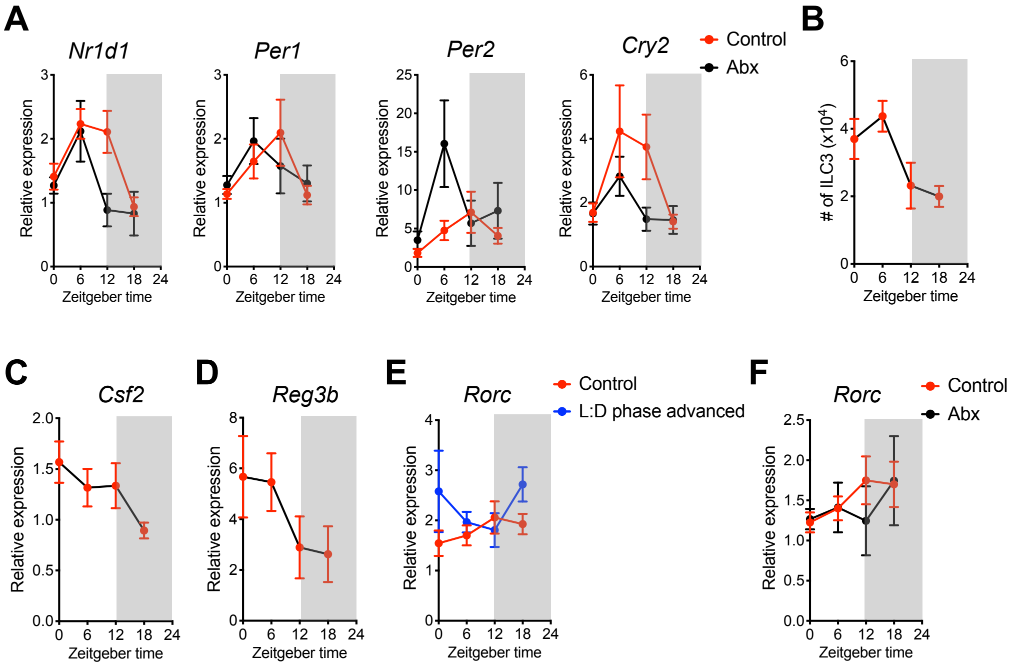

Figure S2. Circadian regulation of ILC3 by light cues and microbiota-derived signals. A. qPCR analyses of indicated genes on sort-purified ILC3 from SI-LP of conventionally housed C57BL/6 mice or mice treated with Abx for 2 weeks. Both groups of mice were sacrificed at ZT0, ZT6, ZT12 and ZT18 within a 24-hour cycle. The gene expression at each time point was first normalized to *Actb2*, then further normalized to the sample with lowest expression at ZT0 within each group (n=6/group, pooled from 2 independent assays). **B.** Isolation of ILC3 from SI-LP of C57BL/6 mice sacrificed at ZT0, ZT6, ZT12 and ZT18 within a 24-hour cycle (n=6, pooled from 2 independent assays). **C.** qPCR analysis of *Csf2* expression on sort-purified ILC3 from SI-LP of C57BL/6 mice sacrificed at ZT0, ZT6, ZT12 and ZT18 within a 24-hour cycle. The relative gene expression was normalized as Fig. 1C (n=6, pooled from 2 independent assays). **D.** qPCR analysis of *Reg3b* expression on small intestinal epithelial cells from C57BL/6 mice sacrificed at ZT0, ZT6, ZT12 and ZT18 within a 24-hour cycle. The relative gene expression was normalized as Fig. 1C (n=6, pooled from 2 independent assays). **E.** qPCR analysis of *Rorc* expression on sort-purified ILC3 from SI-LP of C57BL/6 mice housed in standard light:dark cycle or mice housed in 9-hour advanced light:dark cycle, both groups of mice were sacrificed at ZT0, ZT6, ZT12 and ZT18 within a 24-hour cycle. The relative gene expression is calculated as Fig. 1D (n=6/group, pooled from 2 independent assays). **F.** qPCR analysis of *Rorc* expression on sort-purified ILC3 from SI-LP of conventionally housed C57BL/6 mice or mice treated with Abx for 2 weeks. Both groups of mice were sacrificed at ZT0, ZT6, ZT12 and ZT18 within a 24-hour cycle. The relative gene expression is calculated as Fig. S2A (n=6/group, pooled from 2 independent assays). Results are shown as the mean ± s.e.m.

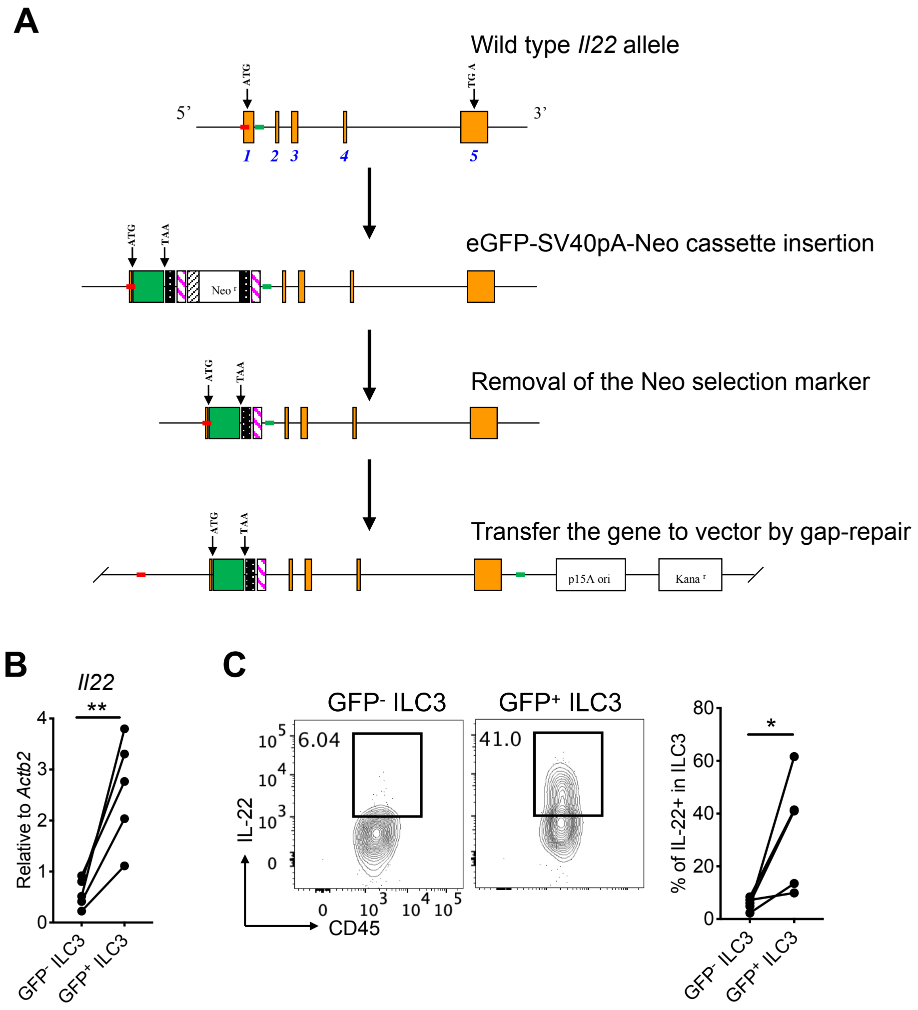

Figure S3. Construct design and experimental validation of BAC transgenic IL-22-eGFP reporter mice. A. On a bacterial artificial chromosome, an eGFP construct was inserted downstream of exon 1 within the *Il22* locus. **B.** qPCR analysis of *Il22* expression on sort-purified GFP$^-$ ILC3 and GFP$^+$ ILC3 from SI-LP of IL-22-eGFP mice. The gene expression was normalized to *Actb2* (n=5, pooled from 2 independent assays). **C.** Representative flow cytometry plots and bar graph of frequency of IL-22$^+$ cells from sort-purified GFP$^-$ ILC3 and GFP$^+$ ILC3 after 4-hour *in vitro* re-stimulation with PMA and Ionomycin. Cells were gated as Fig. 2C (n=5, pooled from 2 independent assays). Statistics are calculated by paired two-tailed Student's *t*-test.

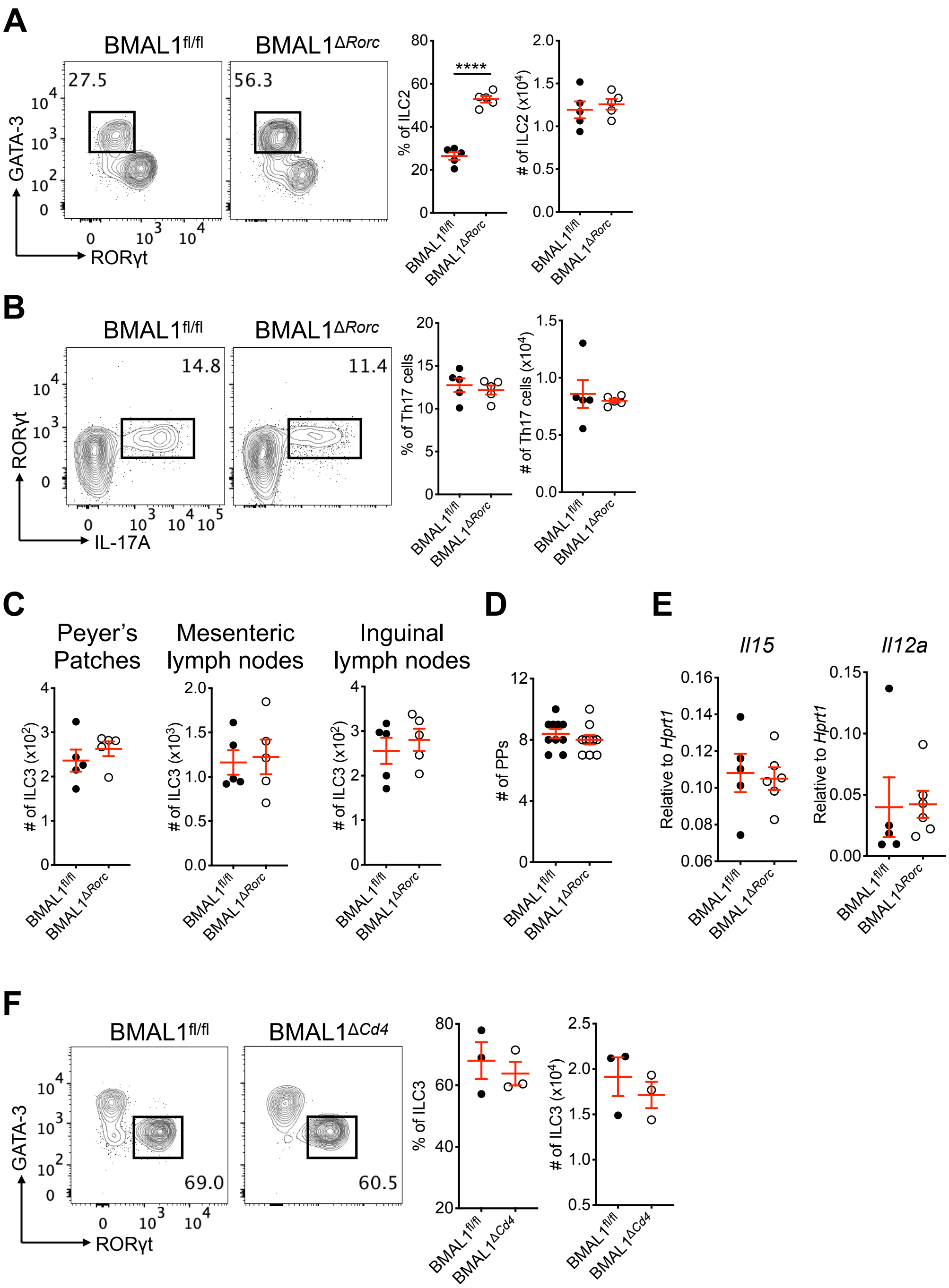

Figure S4. BMAL1$^{\Delta Rorc}$ mice have intact ILC2 and Th17 cell responses in the intestine, and similar cellularity of ILC3 in lymphoid tissues. A and **B.** Representative flow cytometry plots and bar graphs of frequency and cell numbers of SI-LP ILC2 (**A**) and Th17 cells (**B**) from BMAL1$^{fl/fl}$ mice and BMAL1$^{\Delta Rorc}$ mice. Cells were gated on live CD45$^+$Lin$^-$CD90.2$^+$CD127$^+$ for ILC2 and CD45$^+$CD3ε^+CD4$^+$ for Th17 cells (representative of 4 independent assays). **C**. Bar graphs of cell numbers of ILC3 in Peyer's Patches, mesenteric lymph nodes, inguinal lymph nodes from BMAL1$^{fl/fl}$ mice and BMAL1$^{\Delta Rorc}$ mice (representative of 4 independent assays). **D**. Bar graphs of Peyer's Patch numbers from small intestine of BMAL1$^{fl/fl}$ mice and BMAL1$^{\Delta Rorc}$ mice (n=10, pooled from 3 independent assays). **E.** qPCR analyses of *Il15* and *Il12a* expression on sort-purified CD11c$^+$CD11b$^+$ myeloid cells from SI-LP of BMAL1$^{fl/fl}$ mice and BMAL1$^{\Delta Rorc}$ mice. The expression of each target gene was normalized to *Hprt1* (representative of 2 independent assays). **F.** Representative flow cytometry plots and bar graphs of frequency and cell numbers of SI-LP ILC3 from BMAL1$^{fl/fl}$ mice and BMAL1$^{\Delta Cd4}$ mice. Cells were gated as Fig. 3C. Results are shown as the mean ± s.e.m. Statistics are calculated by unpaired two-tailed Student's *t*-test.

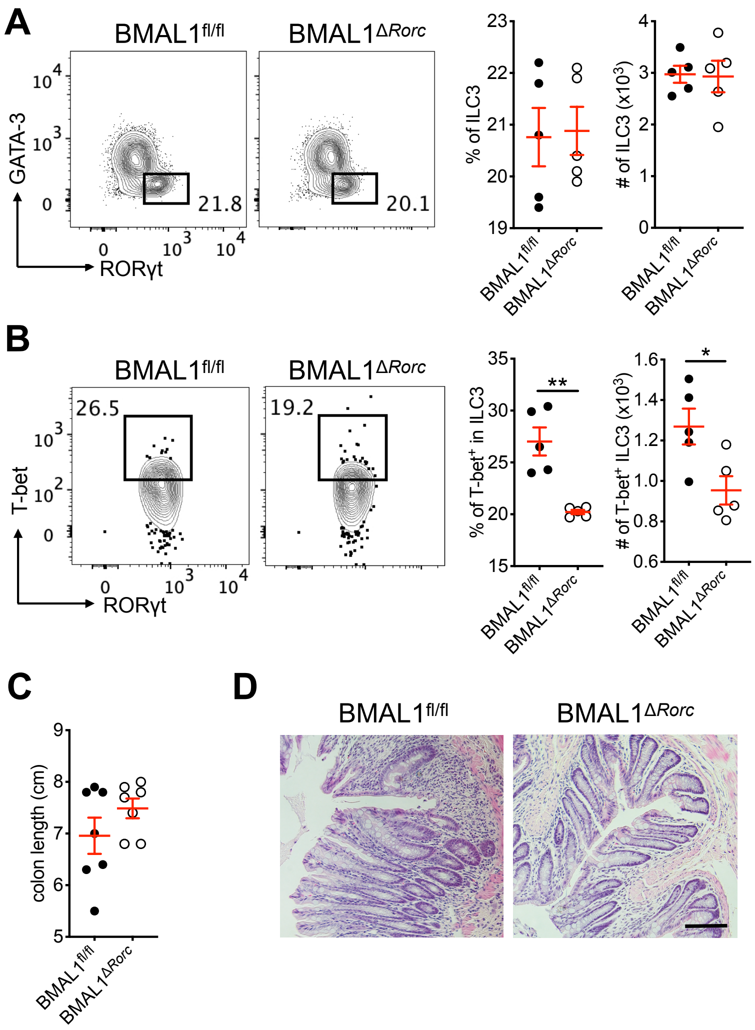

Figure S5. BMAL1 deficiency impacts T-bet^{+} ILC3 in the large intestine. A. Representative flow cytometry plots and bar graphs of frequency and cell numbers of LI-LP ILC3 from BMAL1$^{fl/fl}$ mice and BMAL1$^{\Delta Rorc}$ mice. Cells were gated as Fig. 3C (representative of 4 independent assays). **B.** Representative flow cytometry plots and bar graphs of frequency and cell numbers of T-bet^{+} ILC3 from LI-LP of BMAL1$^{fl/fl}$ mice and BMAL1$^{\Delta Rorc}$ mice. Cells were gated as Fig. 3D (representative of 4 independent assays). **C**. Bar graph of colon length of BMAL1$^{fl/fl}$ mice and BMAL1$^{\Delta Rorc}$ mice at day 13 after administration of DSS (pooled from 2 independent assays). **D**. Representative H&E staining sections of distal colon from BMAL1$^{fl/fl}$ mice and BMAL1$^{\Delta Rorc}$ mice at day 13 after administration of DSS. The scale bar represents 100µm. Results are shown as the mean ± s.e.m. Statistics are calculated by unpaired two-tailed Student's *t*-test.

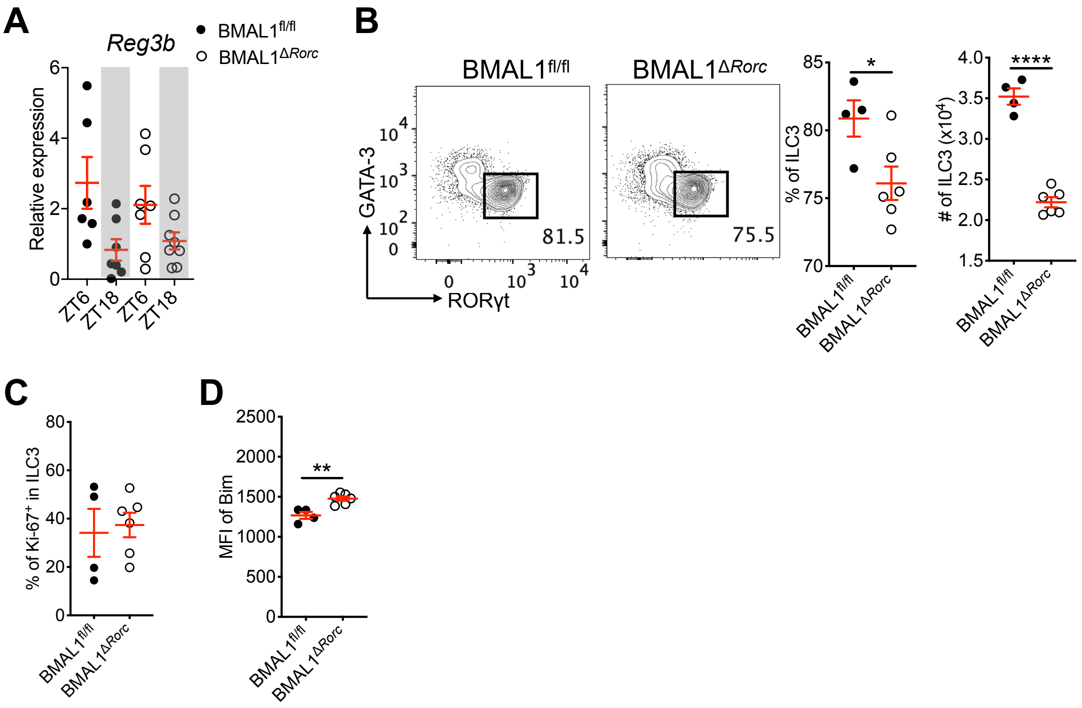

Figure S6. BMAL1 deficiency impairs intestinal ILC3 at weaning. A. qPCR analysis of *Reg3b* on small intestinal epithelial cells from BMAL1$^{fl/fl}$ mice and BMAL1$^{\Delta Rorc}$ mice. Both groups of mice were sacrificed at ZT6 and ZT18. The relative gene expression was normalized as Fig. 4D (n=6-8/group, pooled from 2 independent assays). **B.** Representative flow cytometry plots and bar graphs of frequency and cell numbers of SI-LP ILC3 from 4 weeks old BMAL1$^{fl/fl}$ mice and BMAL1$^{\Delta Rorc}$ mice. Cells were gated as Fig. 3C (representative of 2 independent assays). **C** and **D.** Bar graphs of frequency of Ki-67^{+} ILC3 **(C)** and MFI of Bim expression in ILC3 **(D)** from SI-LP of 4 weeks old BMAL1$^{fl/fl}$ mice and BMAL1$^{\Delta Rorc}$ mice (representative of 2 independent assays). Results are shown as the mean ± s.e.m. Statistics are calculated by unpaired two-tailed Student's *t*-test.

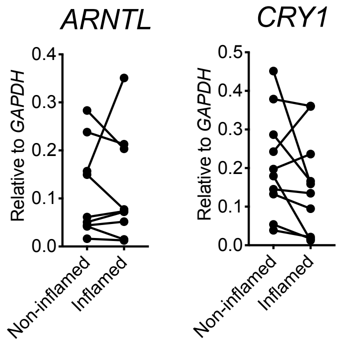

Figure S7. Analysis of circadian genes in intestinal ILC3 from IBD patients. qPCR analyses of indicated circadian genes on sort-purified ILC3 from distal non-inflamed versus matched inflamed surgical resection tissues of IBD patients. The expression of each target gene was normalized to *GAPDH*.

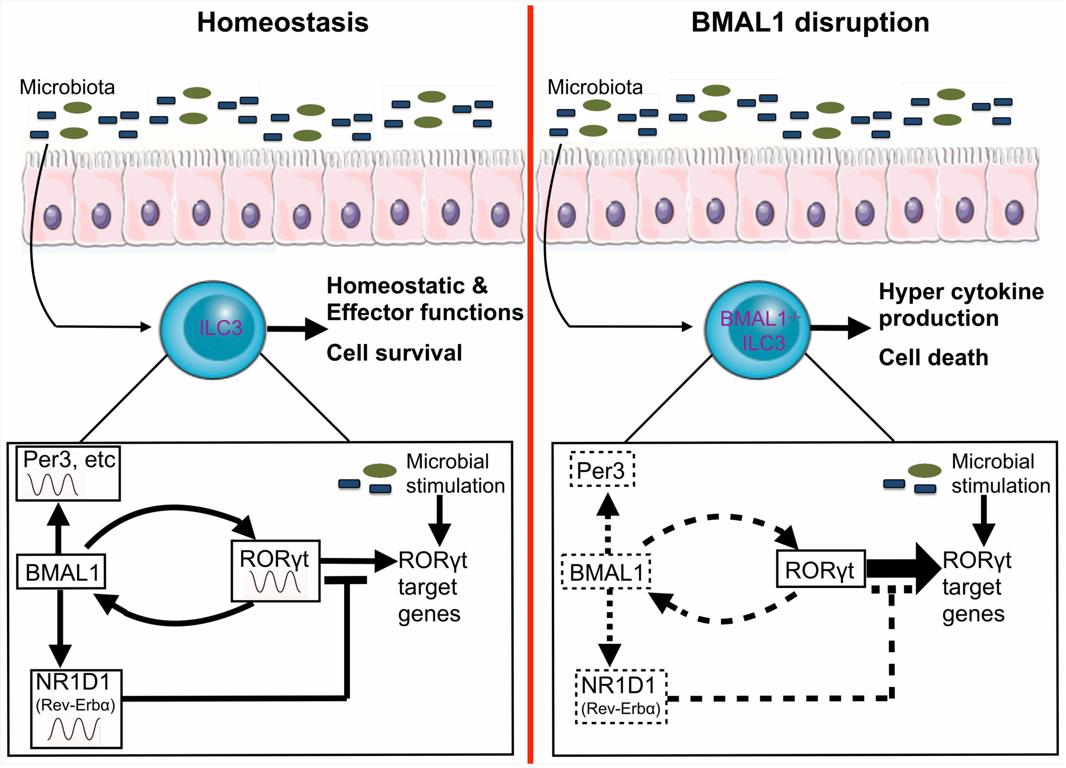

Figure S8. A circadian clock is essential for homeostasis of group 3 innate lymphoid cells in the gut. ILC3 exhibit a cell-intrinsic circadian clock that is required for normal gene expression and homeostasis in the presence of a complex microbiota. ILC3-specific BMAL1 was required for Per3 and NR1D1 expression, fine-tuning of RORγt-mediated transcription in response to microbiota-derived signals, and maintenance of cellular homeostasis. In the absence of cell-intrinsic BMAL1, ILC3 exhibit impaired expression of Per3 and NR1D1, hyper-activation of RORγt-dependent target genes in response to the microbiota, and cell death. Thus, the circadian regulation is essential for homeostasis of ILC3 with the microbiota, and this becomes disrupted in the context of IBD.

Disease type	Age when collected	Sex	Race/Ethnicity	Antibiotic, currently	Antibiotic, ever	anti-TNF treatment, currently	anti-TNF treatment, ever
Crohn's	24	M	Caucasian	Yes	Yes	No	No
Crohn's	39	M	Caucasian	Yes	Yes	No	Yes
Crohn's	57	M	NA	Yes	Yes	No	Yes
Crohn's	26	F	Caucasian	Yes	Yes	Yes	Yes
Crohn's	31	F	NA	Yes	Yes	Yes	Yes
Crohn's	33	F	Caucasian	Yes	Yes	No	Yes
Crohn's	35	F	Hispanic	Yes	Yes	Yes	Yes
Crohn's	37	F	Caucasian	No	No	No	Yes
Crohn's	56	F	NA	No	Yes	Yes	No
Ulcerative Colitis	36	M	Caucasian	NA	Yes	No	No

NA: not available

Table S1. Clinical metadata associated with the human samples.

Primers	**Sequence (5' to 3') or catlog number**
Actb2 (mouse)	Qiagen QT01136772
Nr1d1 -forward (mouse)	TACATTGGCTCTAGTGGCTCC
Nr1d1 -reverse (mouse)	CAGTAGGTGATGGTGGGAAGTA
Per1 -forward (mouse)	TTCGTGGACTTGACACCTCTT
Per1 -reverse (mouse)	GGGAACGCTTTGCTTTAGAT
Cry2 -forward (mouse)	CACTGGTTCCGCAAAGGACTA
Cry2 -reverse (mouse)	CCACGGGTCGAGGATGTAGA
Nfil3 -forward (mouse)	CTTTCAGGACTACCAGACATCCAA
Nfil3 -reverse (mouse)	GATGCAACTTCCGGCTACCA
Arntl -forward (mouse)	AACCTTCCCGCAGCTAACAG
Arntl -reverse (mouse)	AGTCCTCTTTGGGCCACCTT
Per2 -forward (mouse)	CACACTTGCCTCCGAAATAACTC
Per2 -reverse (mouse)	AGCGCACGGCTGTCTGA
Per3 -forward (mouse)	AAAAGCACCACGGATACTGGC
Per3 -reverse (mouse)	GGGAGGCTGTAGCTTGTCA
Rorc (mouse)	Qiagen QT00197722
Il22 -forward (mouse)	GCTCAGCTCCTGTCACATCA
Il22 -reverse (mouse)	CAGTCCCCCAATCGCCTTGA
Reg3b (mouse)	Qiagen QT00239302
Il17a (mouse)	Qiagen QT00103278
Csf2 (mouse)	Qiagen QT00251286
Il15 -forward (mouse)	ACATCCATCTCGTGCTACTTGT
Il15 -reverse (mouse)	GCCTCTGTTTTAGGGAGACCT
Il12a (mouse)	Qiagen QT01048334
Hprt1 -forward (mouse)	CTTGCTGGTGAAAAGGACCTCTC
Hprt1 -reverse (mouse)	GAAGTACTCATTATAGTCAAGGGCA
GAPDH -forward human)	GGAGCGAGATCCCTCCAAAAT
GAPDH -reverse (human)	GGCTGTTGTCATACTTCTCATGG
NR1D1 (human)	Qiagen QT00000413
PER3 (human)	Qiagen QT00097713
NFIL3 (human)	Qiagen QT00013944
ARNTL (human)	Qiagen QT00011844
CRY1 (human)	Qiagen QT00025067

Table S2. Primers used in the study.